High Frequency SSVEP-BCI With Hardware Stimuli Control and Phase-Synchronized Comb Filter

Anna Chabuda, Piotr Durka, and Jarosław Żygierewicz

***Abstract*— We present an efficient implementation of brain–computer interface (BCI) based on high-frequency steady state visually evoked potentials (SSVEP). Individual shape of the SSVEP response is extracted by means of a feedforward comb filter, which adds delayed versions of the signal to itself. Rendering of the stimuli is controlled by specialized hardware (BCI Appliance). Out of 15 participants of the study, nine were able to produce stable response in at least eight out of ten frequencies from the 30–39 Hz range. They achieved on average 96±4% accuracy and 47±5 bit/min information transfer rate (ITR) for an optimized simple seven-letter speller, while generic full-alphabet speller allowed in this group for 89±9% accuracy and 36±9 bit/min ITR. These values exceed the performances of high-frequency SSVEP-BCI systems reported to date. Classical approach to SSVEP parameterization by relative spectral power in the frequencies of stimulation, implemented on the same data, resulted in significantly lower performance. This suggests that specific shape of the response is an important feature in classification. Finally, we discuss the differences in SSVEP responses of the participants who were able or unable to use the interface, as well as the statistically significant influence of the layout of the speller on the speed of BCI operation.**

***Index Terms*— Brain-computer interface, SSVEP, BCI Appliance, comb filter.**

I. Introduction

BRAIN Computer Interface (BCI) is a non-muscular communication pathway, commonly based upon electroencephalogram (EEG).

Steady state visually evoked potential (SSVEP, [1]) is the response of the brain to regularly flickering light, observed in the EEG signal over visual areas of the scalp. SSVEP is frequency-following, its spectrum exhibits characteristic peaks in the stimulation frequency and its harmonics, stable over time [2]. Apart from these purely spectral properties, SSVEP is phase-locked to the stimulus and has a specific, subject-dependent structure, reflected in specific ratios of the harmonic components [3]. Contrary to the spectral properties of SSVEP, it's non-sinusoidal shape—which causes the presence of harmonics—has not been so far explored directly in the construction of a BCI.

SSVEP responses have been measured for stimulation frequencies from 4 to 90 Hz [4]. This broad range is usually divided into three bands: low (below 12 Hz), medium (12–30 Hz) and high frequency (above 30 Hz) [4]. It is easier to detect the SSVEP generated by lower frequency stimuli, because with the increase of frequency the amplitude of SSVEP decreases, and for medium and high frequency bands the EEG spectrum is often corrupted with broad-band muscle artifacts. Therefore the majority of reported SSVEP-based BCIs utilize the low and medium bands [5], [6]. However, SSVEP at these frequencies interfere with the alpha rhythm and can trigger an epileptic seizure in vulnerable subjects [7]. Moreover, the light flickering at low or medium frequencies causes fatigue of subjects attending to such stimuli. In contrast, the high frequency SSVEP-BCI offers a more comfortable, stable and safe system [8]. Nevertheless, there are very few studies of the BCI in the high frequency range, probably due to technical difficulties in implementation of such systems, in terms of both stable and flexible rendering of the stimuli as well as reliable detection of the response.

In this paper we propose a novel SSVEP-based BCI which makes a direct use of the phase relations between the stimuli and SSVEP responses. Characteristic shape of an individual SSVEP response is extracted by a phase-synchronized feedforward comb filter, which adds delayed versions of the signal to itself.

Stimuli for high frequency SSVEP are rendered on the BCI Appliance, which is a hardware device developed since 2009 at the University of Warsaw. In 2012 a compact, wireless version of the BCI Appliance was presented at CeBIT computer fair in Hannover (Figure 1). For the present study, we added to this device an option of monitoring each of the eight active fields with photodiode, as explained in the next section.

II. Materials and Methods

A. Experimental Setup and Data Acquisition

BCI Appliance [9] used in this study consists of liquid crystal display (LCD) backlit by an array of LEDs. The display contains two types of fields. A status field 22.2 cm × 3.8 cm at the top of the screen is used to display non-flickering

Manuscript received October 7, 2016; revised February 27, 2017 and June 7, 2017; accepted July 9, 2017. Date of publication September 28, 2017; date of current version February 9, 2018. This work was supported in part by the Polish Ministry of Science and Higher Education via the Diamond Grant (Diamentowy Grant) Programme under Grant 0159/DIA/2014/43 and in part by the Polish Funds for Science. *(Corresponding author: Anna Chabuda.)*

The authors are with the Faculty of Physics, University of Warsaw, 02-093 Warsaw, Poland (e-mail: anna.chabuda@fuw.edu.pl).

Digital Object Identifier 10.1109/TNSRE.2017.2734164

Fig. 1. **BCI Appliance** presented at CeBIT 2012. Left picture: battery-powered Appliance and EEG amplifier mounted on a chair, with signal displayed on the big screen for demonstration via wireless connection. Right: display of the Appliance during a spelling task. Symbols are rendered dynamically on the LCD screen, while the flickering of each field is controlled separately by underlaid LEDs.

content. A single stimulus field measures 4.6 cm × 3.2 cm. It is typically observed from about 100 cm, which corresponds approximately to 2.6 degree of visual angle. There are eight stimulus fields below the status field, arranged in a 4 by 2 matrix, spaced 0.8 cm apart. LEDs are driven by a microcontroller, ensuring stable frequency (which can be different for each field) and duty cycle of the light flicker. LCD screen overlaid on top of these LEDs allows for standard rendering of computer graphics in the fields corresponding to underlaid LEDs. In such a way we can render arbitrary symbols or texts, constituting the semantic meaning of stimuli, in the fields with hardware-controlled flickering, additionally monitored by a photodiode. Signals from the photodiodes are synchronized to the auxiliary channels of the EEG amplifier.

EEG was recorded using software from BrainTech Ltd., Porti7 amplifier from TMSI and a cap with eight water-based electrodes [10] placed at occipital and parietal locations corresponding to PO8, O2, O1, PO8, PO2, PO3, Pz, and Cz plus ground electrode placed on the left collarbone. Signals from photodiodes fixed to the stimuli fields were recorded together with EEG via auxiliary inputs of the amplifier. Sampling frequency was 512 Hz, reference at PO8.

Fifteen subjects (age: 20–30; 5 females and 10 males) participated in the study. During the procedures, subject was sitting on a comfortable chair with the BCI Appliance approximately 100 cm from her/his eyes.

B. Experimental Procedures

Tasks for each of the 15 subjects included *offline calibration* and two online BCI's: *7-letter speller* and *full-alphabet speller*.

1) Calibration: Responses to stimulation with frequencies from the testing set A

$$A = \{30, 31, 32, 33, 34, 35, 36, 37, 38, 39\}\,\text{Hz} \qquad (1)$$

were evaluated during the calibration procedure. In this procedure, eight different frequencies $f_1, f_2 \ldots f_8$ were simultaneously flashing on the stimulus-fields of the BCI Appliance. Subjects were asked to concentrate on the field indicated by an asterix. For the given trial, frequency of this field was considered as the target frequency f_T, while the remaining seven frequencies were considered as non-targets, f_{NT}. Each frequency from the set A was used as the target eight times, resulting in 80 recorded trials. Each trial was five seconds long followed by one second break, so the calibration took 8 min.

2) Online Operations: Interface of the BCI Appliance during online tasks is presented in Fig. 2. In both tasks subjects were asked to type via BCI five Polish phrases. In both tasks, participants were supposed to focus on the field (containing a character, a group of characters or a command) they wanted to select. Right after selection, there was one-second break for a feedback, during which the selected field turned green. The phrase to spell and all characters selected so far were displayed on the status-field. To continue to the next phrase the subject had to finish spelling the current phrase correctly. In both tasks, the order in which phrases were presented was random.

a) 7-letter speller: Participants were asked to spell words: *tablica*, *trofeum*, *uśmiech*, *uniform*, *wiadukt*. Each word had seven characters. To make the task as simple as possible, only the characters that were included in the currently spelled word were displayed on the stimulus-fields, and they were in the correct order. The command *delete* was displayed on the last field (Fig. 2 a)).

b) Full-alphabet speller: This task was more complicated, because the interface had been switched to two-level mode, giving access to the full alphabet. Seven groups of characters and the command *delete* were displayed in the first level of the interface, choosing a group led to the second level where letters from that group and command *back* were presented (Fig. 2 b)). In the full-alphabet speller, participants were asked to spell phrases: *bci* (3 characters-long), *fizyk* (5 characters-long), *rysunek* (7 characters-long), *interfejs* (9 characters-long), *interfejs mózg-komputer* (23 characters-long) using the two-level interface.

The experimental protocol was approved by the Rectors Committee for Ethics of Research with Human Participants (at the University of Warsaw).

C. EEG Signal Processing

The experiment was divided into two parts: calibration and online tasks (7-letter speller and full-alphabet speller). Signal processing pipeline for the calibration consisted of:

1) estimation of spatial filter,
2) estimation of temporal patterns,

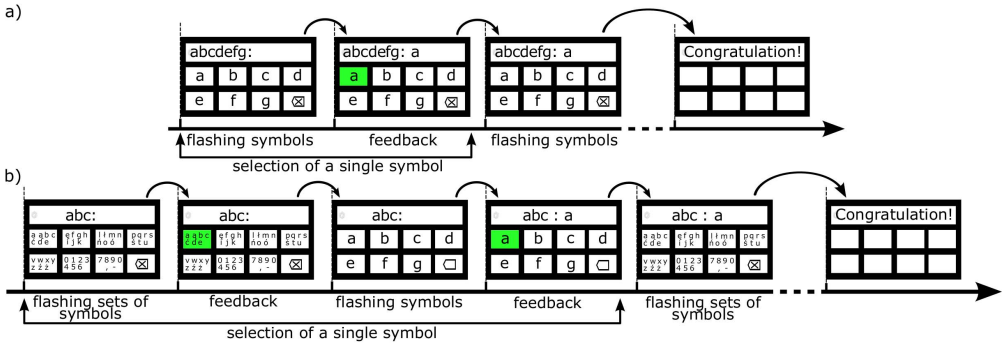

Fig. 2. **Schemes of the online procedures**. (a) 7-letter speller, (b) full-alphabet speller. In both tasks, participant had to spell five phrases. To select a character in the first task (a), he or she just had to focus on the field with the character. Selection in the second task (b) required passing two levels of the interface: first focus on the field with the group containing the character (selection of the group), and then focus on the field with the character (selection of the character).

3) evaluation of features,
4) selection of the best subset of stimulation frequencies,
5) estimation of parameters of the classifier.

and for online spellers:

1) preprocessing of signal buffer,
2) estimation of candidates temporal patterns,
3) classification of candidates temporal patterns.

Following paragraphs describe some of the signal processing methods and their roles in these tasks.

1) Spatial Filtering: Common spacial pattern (CSP) [11] is a mathematical procedure for spatial filtering of multivariate signals. The objective is to find a linear combination of measured signals such that it has maximal variance for the subset of data from one experimental condition and minimal variance for the subset from the other experimental condition. The optimization problem is equivalent to maximizing the Rayleigh quotient $r(\mathbf{w})$:

$$r(\mathbf{w}) = \frac{\mathbf{w}^T \mathbf{R}_T \mathbf{w}}{\mathbf{w}^T \mathbf{R}_{NT} \mathbf{w}} \tag{2}$$

where: $\mathbf{R}_T$ is the covariance matrix of the subset of data for which one wants to maximize the variance (the target subset), and $\mathbf{R}_{NT}$ is the covariance matrix of the subset of data for which one wants to minimize the variance (the non-target subset)

The solution of the optimization problem can be obtained by solving the generalized eigenvalue problem. The CSP filtering is done by projecting data in the direction of the vector $\mathbf{w}^*$ which maximizes the quotient. Because of the expected increase of power at the stimulation frequency, the method can be applied to separate SSVEP from ongoing spontaneous activity.

In the current study, signal recorded during calibration procedure was used to estimate CSP filter. The matrices $\mathbf{R}_T$ and $\mathbf{R}_{NT}$ are of the size 7×7 (7 is the number of active channels), and are estimated as $\mathbf{R} = \mathbf{S}\mathbf{S}^T$ averaged over the trials, where $\mathbf{S}$ is the target or nontarget signal from a single epoch, respectively. The target signals were obtained by filtering the 5s-long epochs of EEG recorded during stimulation with target frequency f_T with Chebyshev type II bandpass filter (order 1) centered on the stimulation frequency f_T. The non-target signals were obtained by filtering the same 5s-long epochs of EEG with Chebyshev type II bandpass filter (order 1), but centered on a different frequency f_{NT} (from the set A).

2) Temporal Patterns and Features for Classification: CSP-filtered signals $\mathbf{s}$ of length L_b were normalized to have norm equal to 1 and used to compute the temporal patterns of length L_p. The procedure is outlined in Fig. 3. For a given frequency F, m indices $k_1, \ldots, k_m$ of samples corresponding to the onset of the flash were determined from the auxiliary signals recorded from photodiodes. These indices were used to extract and align epochs of length L_p:

$$\mathbf{s}_i^F = \mathbf{s}\,[k_i : k_i + L_p], \quad i \in \{1, \ldots, m\} \text{ and } m + L_p < L_b \tag{3}$$

In this study we used $L_b = 3\,\text{s}$ and $L_p = 1\,\text{s}$. The pattern $\mathbf{p}^F$ is computed by averaging aligned signal epoch $\mathbf{s}_i^F$:

$$\mathbf{p}^F = \frac{1}{m} \sum_{i=1}^{m} \mathbf{s}_i^F \tag{4}$$

This procedure corresponds to a feedforward comb filter [12] with gain equal to 1 and delays equal to the stimulation period, but in this case adjusted by hardware so that the delayed signals always start at the beginning of each flash. Each of the eight flashing frequencies can be used for indexing and aligning.

In the calibration session the target frequency f is known for each trial, therefore we can form a target pattern $\mathbf{p}_T^F$, if $F = f$. The target patterns $\mathbf{p}_T^F$ are further averaged across all respective calibration trials to form the reference patterns $\hat{\mathbf{p}}_T^F$.

In the online session, the target frequency is unknown (it is to be determined), therefore we form candidate patterns $\mathbf{p}_C^F$ for all possibles frequencies. The feature, used in this study, was the Pearson correlation coefficient between the patterns: $r(\hat{\mathbf{p}}_T^F, \mathbf{p}_C^F)$.

3) Selection of Optimal Stimulation Frequencies: The set of considered candidate stimulation frequencies A, mentioned in section "Calibration", contains 10 frequencies, while the BCI-Appliance has only 8 stimulus fields. Therefore eight frequencies, yielding the best responses, were chosen for each user by means of the following procedure:

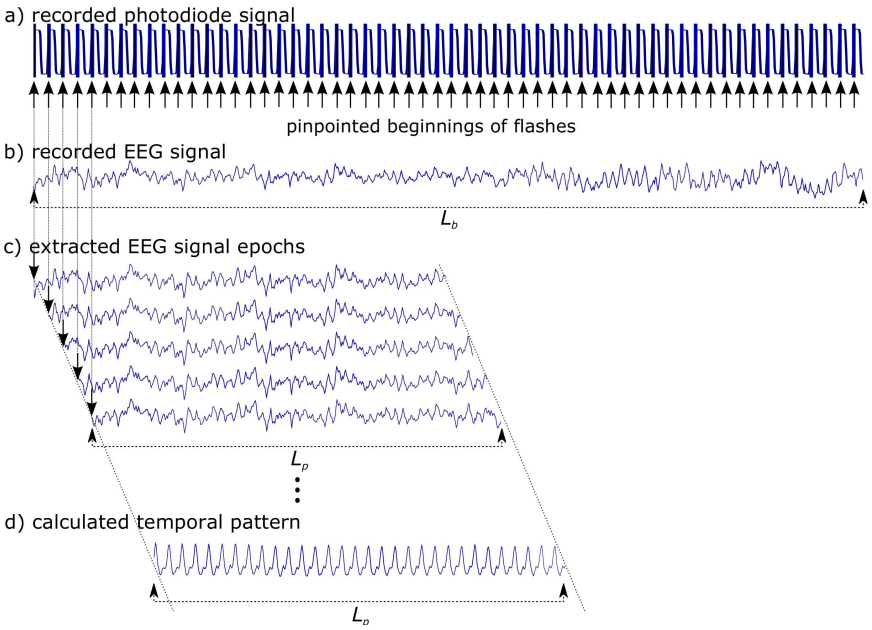

Fig. 3. **Scheme of computing the temporal pattern.** (a) photodiode signal (b) EEG signal (c) extracted EEG signal epochs (d) calculated response pattern. The response pattern (d) is computed by averaging all aligned L_p-long signal epochs (c) extracted from L_b-long signal. (b) Starting points of epochs (c) correspond to the rising slopes of the photodiode signal (a).

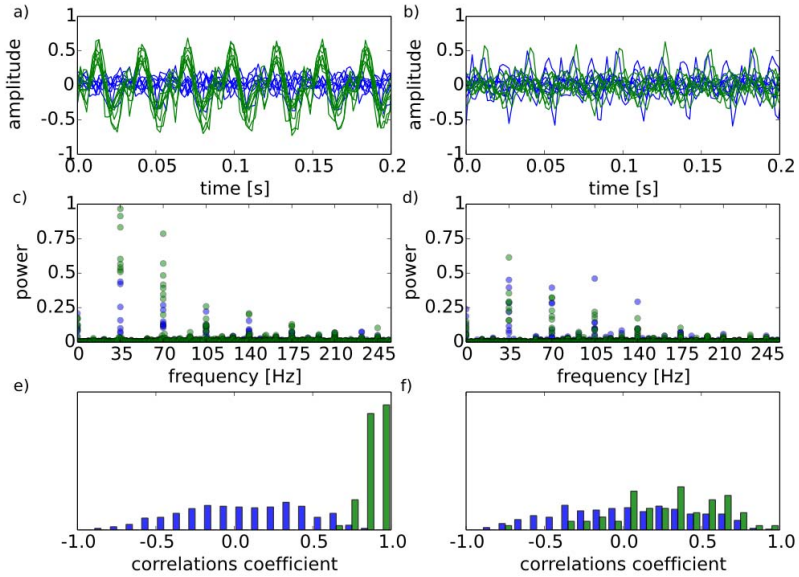

Fig. 4. **Calibration results for 35 Hz stimulation for two subjects**. a) and b) overlaid fragments of candidate pattens from eight realizations of stimulation. c) and d) power spectra of the patterns. e) and f) distributions of the correlation coefficients ρ_T^F and ρ_{NT}^F. Green – results from target data, blue from non-target data. Left column – data from one of the subjects who completed both tasks, right column – data from one of the subjects who failed.

Each calibration trial i was divided into: 3s-long reference signal $\mathbf{x}_i$ and 2s-long test signal $\mathbf{y}_i$. A set of candidate test patterns $\mathbf{p}_{C,i}^F$ was computed from the $\mathbf{x}_i$, and the target reference patterns $\hat{\mathbf{p}}_T^F$ were computed from the $\mathbf{y}_i$, for each frequency F in set A. These patterns were used to compute two distributions of the correlation coefficient (illustrative distributions are depicted in Fig.4 e) and f)):

- $\rho_T^F = \left\{ r(\hat{\mathbf{p}}_T^f, \mathbf{p}_{C,i}^F) \right\}$, where candidate patterns were these with target frequency stimulation ($F = f$)
- $\rho_{NT}^F = \left\{ r(\hat{\mathbf{p}}_T^f, \mathbf{p}_{C,i}^F) \right\}$, where candidate patterns were these with non-target frequency stimulation ($F \neq f$)

These distributions were used to compute the ROC curve for each frequency F. The ROC curve was created by plotting the true positive rate (TPR) against the false positive rate (FPR) at various thresholds of correlation coefficient. In this case TPR was computed as a fraction of cases in the set ρ_T^F above the threshold. FPR was computed as a fraction of cases in the set ρ_{NT}^F above the threshold. We used area under that curve (AUC) as the measure of the quality of the feature ($r(\hat{\mathbf{p}}_T^F, \mathbf{p}_C^F,)$) [13]. The frequencies yielding the largest AUC were selected for online stimulation.

4) Target and Non-Target Distributions: The distributions ρ_T^F, for the selected frequencies F, were pooled together and

yielded the target distribution ρ_T in order to improve the estimation of probabilities required by the classifier. Similarly, the ρ_{NT}^F distributions were pooled to form the non-target distribution ρ_{NT}.

5) Online Analysis and Classification: In the online mode the signal was buffered in a 3 s long FIFO buffer. After each $\Delta t = 0.2$ s the buffered epoch was processed in the following way. The signal was detrended by subtracting the mean, and notch-filtered to remove the line noise. Next it was projected by the CSP filter. Then it was aligned and averaged according to the events obtained from the stimulation-fields signals, to form the eight candidate temporal-patterns $\mathbf{p}_C^{F_i}$, $i = 1, \ldots, 8$, each corresponding to one of the stimulation frequencies. These patterns were correlated with the reference target patterns corresponding to the same frequency, to yield the classification feature $r_i = r(\hat{\mathbf{p}}_T^{F_i}, \mathbf{p}_C^{F_i})$.

The value of the feature was used by a naive Bayes classifier [14] to assign target or non-target class to the feature r_i.

$$\text{class}_i = \underset{k \in \{T, NT\}}{\text{argmax}} \left(P(r_i|k) P(k) \right) \tag{5}$$

where $P(k)$ is the probability of class k, and $P(r_i|k)$ is the probability of r_i in class k.

If the classifier labeled only one of the features as belonging to the target class, the corresponding decision was generated and passed to the BCI appliance. If none or more than one feature was labeled as target, the appliance waited Δt to make next attempt to classify the signal.

D. Analyses of Efficacy

1) Rules for Computation of the Information Transfer Rate: Prior to computing the information transfer rate (ITR), strict rules were formulated:

1) Participant's data were included in evaluation of ITR and accuracy only if all words from both online tasks were successfully spelled.
2) ITR was calculated on the basis of selected commands. In every step there were 8 available commands.
3) Correct command is defined as a command that, chosen out of all other commands available in given step, enables the user to fulfill the task in the least possible number of steps, i.e.: selecting a correct or deleting an incorrect letter/group of letters, or returning from an incorrectly chosen group of letters. All commands in a given state, not fitting above mentioned definition, are considered to be incorrect commands, i.e.: selecting an incorrect or deleting a correct letter/group of letters, or returning from the correct group of letters before choosing one.

2) Information Transfer Rate and Accuracy: Information transfer rate and accuracy were computed to check the usability and efficiency of the proposed system. Accuracy was computed as the ratio of of the number of correct commands to the number of all commands selected, expressed as percentage.

ITR was calculated as a product of the number of selections per minute and the number of bits per command B, based on the following formula [15]:

$$B = \log_2 N + P \log_2 P + (1 - P) \log_2 \frac{1 - P}{N - 1} \tag{6}$$

where: N is the total number of possible commands (in this study 8), and P is the probability of correct selection calculated as the ratio of the number of correct commands to the number of all commands selected.

3) Evaluation of Parametrization: Parametrization of SSVEP in terms of Signal-to-Noise-Ratio (SNR) was proposed in [16] and used e.g. in [3] and [9]. SNR measures the power at a given stimulation frequency (regarded as signal level) with respect to the mean level of power in adjacent frequencies (regarded as noise level). It was calculated as:

$$\text{SNR}_i^F = \frac{\sum_{j=-2}^{2} P(F + j\Delta f)}{\sum_{j=4}^{5} \left(P(F + j\Delta f) + P(F - j\Delta f) \right)} \tag{7}$$

where $P(F)$ is spectral power at frequency F and $\Delta f = 0.1$ Hz. It was computed for 2s long epochs extracted from calibration trials, 2 epochs from each trial. The trials were preprocessed (i.e. frequency and spatially filtered) in the same way as for the computation of spatial patterns. Power was estimated by means of a periodogram with Blackman window, zero-padded to 5120 samples. Two distributions of SNR_i^F values were formed for each frequency F from set A (1):

- the target distribution, for the cases when F is equal to the actual target stimulation frequency f_T for a given trial,
- the non-target distribution, when for computation of SNR_i^F, a non-target, simultaneously stimulated frequency $F = f_{NT}$ was used.

These distributions were used to compute the ROC curves, by varying the threshold SNR level, and subsequently AUC was derived form the ROC curves.

III. Results

A. Feature Extraction

Illustrative partial results obtained from calibration sessions from two subjects are presented in Fig. 4. Data shown in the left column is from a subject with good performance, in the right column—from a poorly performing subject. Exemplary patterns are depicted in panels a) and b). Panels e) and f) show examples of the distributions of correlation coefficients used to compute AUC.

B. Comparison of Feature Quality

Box-plots in Fig. 5 show the outline of distributions of the AUCs obtained for each participant—AUC obtained for distribution of correlations of temporal patterns, and second for distributions of SNRs. AUC values were obtained for a given subject for her/his eight best frequencies. The AUC values obtained for the feature proposed in this paper were significantly higher than those for SNRs as assessed by means of Wilcoxon signed-rank paired test ($W = 0.0$, $p = 0.001$).

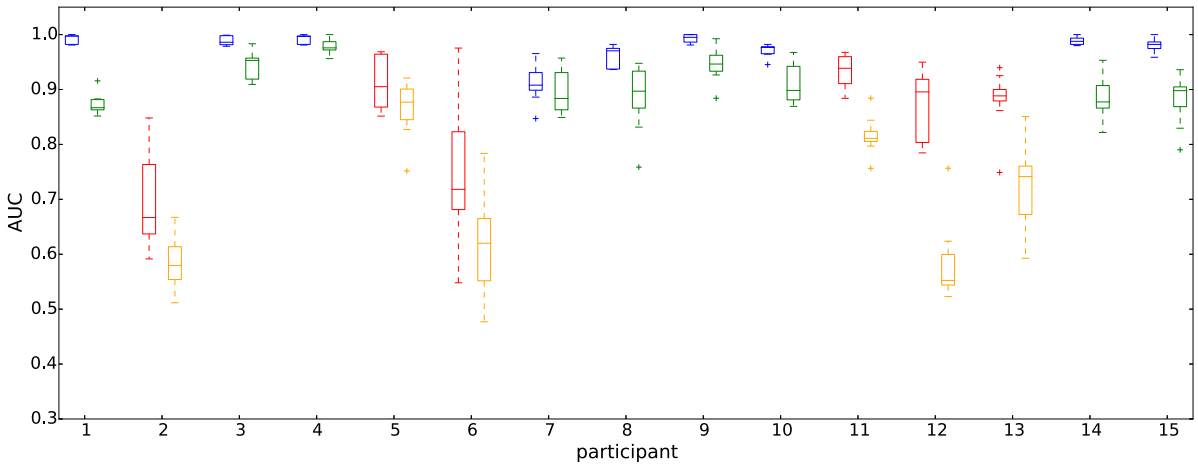

Fig. 5. **AUC observed in calibration**. Each box-plot outlines the distribution of the AUC values obtained for a given subject for his eight best frequencies selected for the online tasks. There are two box-plots for each subject: first (blue or red) for AUC obtained for distribution of correlations of temporal patterns, and second (green or orange) for distributions of SNRs. Color code: blue and green—subjects who passed both tasks; red or orange—subjects who failed in the online tasks.

C. BCI Literacy Results

From the group of 15 participants of this study, 9 were able to complete both tasks. The other six (including Subjects 5 and 11, who had good results in calibration but the signal quality dropped dramatically in the online tasks) could not write the 7-letter words in the first task. Some insight into the problem of BCI-literacy can be obtained from the analysis of calibration data. In Fig. 4, the panels a) and b) show overlaid candidate patterns obtained for several buffers—$\mathbf{p}^{f}_{C,i}$: green, and $\mathbf{p}^{F\neq f}_{C,i}$ blue. In this case $f = 35\,\mathrm{Hz}$. Note the appearance of a repetitive target pattern in the first case, which is clearly distinct from the non-target candidate patterns. In case of a poor performer a clear target pattern is not formed in most of the trials. In panels c) and d) power spectra of the patterns are presented. Note the presence of the fundamental frequency and all the harmonics up to the Nyquist frequency. The most pronounced differences between target and non-target patterns are in fundamental and first harmonics. The bottom panels e) and f) show the empirical distributions of correlation coefficients ρ^{F}_{T} and ρ^{F}_{NT}. In the case of a good performer the distributions have very small overlap, while for the poor performer the distributions overlap in wide range of the feature values.

It is worth to note a clear separation of good and poor performers in terms of the AUC values, indicating that in case of poor performers the distribution of ρ^{F}_{T} and ρ^{F}_{NT} strongly overlap.

Figure 6 summarizes the performance obtained for subjects who were able to complete both tasks. Box-plots in panel a) outline the distributions of time needed to select a single command. Generally, the average time needed in 7-letter speller (3.6±0.2 s) was shorter than in the full-alphabet speller (3.9±0.3 s). This difference is statistically significant—assessed by means of Wilcoxon Signed-rank paired test ($W = 1.0$, $p = 0.028$). This tendency is preserved in the times needed to select a correct command, as seen in panel b); for the 7-letter speller it's 4.29±1.24 s, and for the full-alphabet speller — 4.5±0.7 s; however, this difference is not statistically significant ($W = 8.0$, $p = 0.31$).

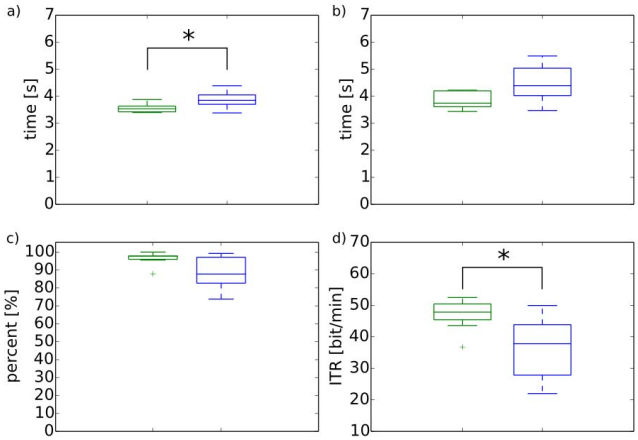

Fig. 6. Results of BCI performance. The results were computed for all participant, who finished both online tasks. (a) average time for selection a single command; (b) average time for selection a single correct command; (c) accuracy; (d) ITR; green—7-letter speller, blue—full-alphabet speller.

TABLE I
ACCURACY [%] IN THE 7-LETTER SPELLER. ACCURACY OF SPELLING OF EACH WORD FOR EACH PARTICIPANT FROM THE BCI-LITERATE GROUP

	Word number					
Subject id	**1**	**2**	**3**	**4**	**5**	**Mean**
1	100	100	89	100	100	**98±4**
3	82	100	100	100	100	**96±7**
4	100	100	100	100	89	**98±4**
7	73	100	100	70	88	**86±13**
8	89	100	100	100	100	**98±4**
9	89	100	100	100	89	**96±5**
10	100	100	100	100	100	**100±0**
14	100	100	100	100	100	**100±0**
15	89	100	100	100	89	**96±5**
Mean	**91±3**	**100**	**99±1**	**97±3**	**96±2**	

Average accuracy achieved in 7-letter task was 96±4% and, as presented in Table I, there were many cases when it

TABLE II
ACCURACY [%] IN THE FULL-ALPHABET SPELLER. ACCURACY OF SPELLING OF EACH WORD FOR EACH PARTICIPANT FROM THE BCI-LITERATE GROUP

	Length of the word					
Subject id	**3**	**5**	**7**	**9**	**23**	**Mean**
1	100	100	78	100	61	**88±16**
3	100	100	96	100	100	**99±2**
4	79	77	78	82	92	**82±5**
7	60	78	74	88	70	**74±9**
8	73	77	78	82	92	**80±6**
9	94	100	89	100	100	**97±4**
10	100	95	92	100	100	**97±3**
14	100	95	92	88	70	**89±10**
15	100	100	96	82	92	**94±7**
Mean	**90±5**	**91±4**	**86±3**	**91±3**	**86±5**	

TABLE III
ITR [BIT/MIN] IN THE 7-LETTER SPELLER. ITR OF SPELLING OF EACH WORD FOR EACH PARTICIPANT FROM THE BCI-LITERATE GROUP

	Word number					
Subject id	**1**	**2**	**3**	**4**	**5**	**Mean**
1	51.4	46.3	35.3	51	52.2	**47.2±6.3**
3	26.3	55.7	51.4	54.4	51.3	**47.8±10.9**
4	57.5	55.8	53	47.8	37.8	**50.4±7.1**
7	23.1	52.3	47.9	27.7	32.8	**36.8± 11.4**
8	33.6	53.4	55.3	54.6	55.7	**50.5±8.5**
9	24.4	55.5	55.8	41.9	40.2	**43.6±11.6**
10	52.5	55.7	52.7	51.1	55.2	**53.4±1.7**
14	52.2	52.8	46.3	47.2	49.2	**49.5±2.6**
15	33.6	52.5	49.2	45.3	41.2	**44.4±6.6**
Mean	**39.4±4.6**	**53.3±1**	**49.7±2.8**	**46.7±2.8**	**46.2±2.8**	

TABLE IV
ITR [BIT/MIN] IN THE FULL-ALPHABET SPELLER. ITR OF SPELLING OF EACH WORD FOR EACH PARTICIPANT FROM THE BCI-LITERATE GROUP

	Length of word					
Subject id	**3**	**5**	**7**	**9**	**23**	**Mean**
1	45.3	52.8	25.3	50.5	15.1	**37.8±14.9**
3	46.8	52.9	47.5	50	42.2	**47.9±3.6**
4	27.5	42.9	21.5	27.2	38.2	**31.5±7.9**
7	13.6	26.3	22.9	29.1	18.1	**22±5.6**
8	20.5	22.4	21.8	21.7	34.8	**24.2±5.3**
9	35.9	43.6	34.1	41.9	44.5	**40±4.2**
10	54.1	41.5	43.2	55.5	55.3	**49.9±6.2**
14	45.6	40.3	40.1	27.8	21.3	**35±9**
15	45.1	40.2	39.2	25.3	35.2	**37±6.6**
Mean	**37.2±5.6**	**40.3±3.4**	**32.8±3.4**	**36.6±4.3**	**33.9±2.8**	

reached 100%. In case of the full-alphabet speller the average accuracy was 89±9%, s presented in Table II. We can see a tendency for lower accuracy in the more difficult task, but in the tested group the difference in accuracy did not reach statistical significance ($W = 4.0$, $p = 0.09$).

The effectiveness of information transfer as measured by ITR is illustrated in panel d). As can be expected from the shorter time to select a command and higher accuracy of selection in the 7-letter speller, ITR in this task (47±5 bit/min) was higher than in the full-alphabet task (36 ±9 bit/min). This difference was statistically significant ($W = 0.0$, $p = 0.001$). The ITR results obtained for each of the subjects in the 7-letter task and the full-alphabet speller task are presented in Tables 3 and 4, respectively.

IV. DISCUSSION

A. Comparison to Other High-Frequency SSVEP-Based BCIs

This section quotes performances reported in recent papers on high-frequency (above 30 Hz) SSVEP-BCIs applied to human subjects. These results are also summarized in Table V.

- SNR, i.e. power of the signal in the stimulated frequency relative to the spectrally-neighboring frequencies, was used as a feature for classification in an offline study [8]. The estimated mean accuracy of 96% was obtained for time windows with duration 4 s; the tested frequency range was 21–43 Hz.
- Canonical correlation analysis (CCA) and SNR-based classification of stimulation frequency was applied to quantify SSVEPs in the range 27–43 Hz in [17]. It was shown that CCA-based BCI is more robust in respect to noise than SNR-based BCI, reaching maximal accuracy of about 75% for 2.25 s time window. In these conditions the SNR classification had about 70% accuracy. Another approach to compute a measure similar to SNR was proposed in [18]. Power relative to baseline, calculated from 2 s time windows was averaged across channels and used as the feature for classification of SSVEP in range 37–40 Hz. The reported ITR was 4 to 45 bits/min and accuracy 65–100%.
- Spatial filters specially tailored to SSVEP can significantly improve the efficiency of a BCI. In [5] a spatial filter was applied to enhance the SSVEP and an unsupervised linear classification was used to detect users intentions. The authors obtained information transfer rate of 12.1±7.3 bits/min and accuracy 89.2±9.3% for time windows with duration 2 s and frequency set: 34, 36, 38, 40 Hz. Using filters based on a model of SSVEP Molina and Mihajlovic [19] reached information transfer rate of 20.9 to 22.7 bits/min for frequencies above 30 Hz.
- In an offline study [20], a spatial filter, similar to [19], was used to enhance SSVEP and phase delay was calculated as a lag between phase of reference stimulation recorded by photodiode and phase estimated for SSVEP. A single frequency from a range between 30 Hz and 40 Hz, which elicited the strongest response for a given subject, was used for stimulation. The reported accuracy, calculated for 1 s time window was 86.5±5.4%.
- In [21] bandpass-filtered epochs were averaged to sharpen the recorded SSVEP. After that, the phase was estimated as lags between the currently measured SSVEP and the SSVEP recorded for stimulation without phase displacement during the calibration. The authors reported accuracy of 83.49±10.4% and ITR of 24.28±6.77 bits/min using 2 s time window.
- Spatial filtering followed by a phase synchrony analysis was used to detect the phase from the recorded SSVEP in [22]. In this case a single frequency from a range between 32 Hz and 40 Hz, which elicited the strongest response for a given subject, was used for stimulation. The authors obtained accuracy of 95.5±7% and an ITR of 34.15±5.57 bits/min, using 1.5 s time window.
- Finally, in [23] authors achieved accuracy 93.5±5.6% and ITR 33.8±8.7 bits/min by using another phase-related technique, which they called multi-phase cycle coding.

TABLE V
HIGH-FREQUENCY SSVEP-BCI REPORTED IN LITERATURE. "SIMPLE" AND "FULL" IN THE "CITATION" COLUMN REFER TO RESULTS OF THIS STUDY FOR THE 7-LETTER AND THE FULL SPELLER, RESPECTIVELY. "USERS" DENOTES THE NUMBER OF THOSE PARTICIPANTS OF THE STUDY WHO SUCCESSFULLY USED THE INTERFACE

Citation	Participants	Users	Freqs [Hz]	#of fields	Type	Key tech. for param. of SSVEP	Accuracy [%]	ITR [bpm]
[8]	13	NA	21–43	NA	offline	SNR	96	NA
[17]	11	NA	27–43	NA	offline	CCA-SNR	70	NA
[21]	7	7	31.25	4	online	single frequency phase delay	83.49	24.28
[18]	6	6	37–40	4	online	power relative to baseline	65–100	4–45
[23]	15	13	37–40	4	online		NA	44.6
[5]	84	56	34–40	4	online	spatial filter	89.16	12
[22]	6	6	32–40	4	online	phase synchrony analysis	95.5	34.15
[24]	8	8	30–40	3	online	multi-phase coding (MPCC)	93.5	33.77
simple	15	9	30–39	8	online	time domain comb filter	96	47
full	15	9	30–39	8	online	time domain comb filter	89	36

- This study: 96±4% accuracy and 47±5 bit/min transfer for a simple 7-letter speller, and 89±9% accuracy and 36±9 bit/min transfer in a full-alphabet speller task.

In the light of above cited results, the efficacy of the system proposed in this study provides a substantial progress; however, the value of this comparison is limited since computations were performed on different datasets form different subjects. To cope with this problem, we performed also a direct comparison of the parametrization of SSVEP response proposed in this work with the SNR feature, by means of AUC evaluated on the same data, with the same preprocessing. The AUC estimated for the calibration data indicates that, independent of the applied classifier, the correlation of time patterns is a better feature for classification than SNR.

B. ITR Dependence on the Simplicity of the Interface Layout

We investigated BCI performance in two tasks: a simple 7-letter speller with letters ordered according to the expected order of selection, and a full-alphabet speller with layout unrelated neither to the task nor to the prior experience of the users, since there are no generic standards for 8-field communication. In this way, using the 7-letter speller, we can measure the properties of the signal processing and classifier algorithms, and minimize the factors related to the task complexity. The full-alphabet speller task is closer to a usable interface, but is more demanding on the user since each letter has to be found on the display.

These expectations are confirmed by the statistically significant difference in times needed to select a symbol in either of these interfaces. The additional time of 0.31 s (on average) in case of full-alphabet speller is needed to find the location of the next symbol to select. With a proper training in using the full-alphabet speller this time might be reduced. It leaves also the space for improvements in the design of the speller interface. The accuracy, although not significantly different in both tasks, decreases slightly in the second task. Prevalence of 100% accuracies in the first task (Tab. I) suggests that the algorithms for command classification work reliably. Taking this into account, large amount of lower accuracies the second task (Tab. II) can be attributed to suboptimal design of the interface of the full-alphabet speller.

Discussed above differences in accuracy and the time of command selection yield significantly different ITRs between the tasks. The theoretical limit in case of current setup with 8 fields (3 bits) and buffer length of 3 s is 60 bits/min, significantly higher than the average result even in the 7-letter task. To investigate the origins of this difference we analyzed the records of classifier states for attempts to classify individual commands. We found that it was very often the case that in the few initial attempts, i.e. those occurring at 3.0, 3.2, and 3.4 seconds after the end of the feedback, the command was not classified because more than one candidate pattern yielded high probability of being the target. It suggests that there is some time needed to focus the attention on the desired stimulus-field after the feedback. During this time the gaze seems to sweep across fields flickering with different frequencies.

C. BCI-Literacy in the Current Study

The BCI-literacy observed in this study is 60%, in concordance with results reported in literature. Quoting from [5], "[...] across different BCI approaches (SSVEP, P300, ERD/ERS), about 20% of users are unable to attain effective control, while about another 30% attain only poor control [...]". More specifically, in case of high-frequency SSVEP-BCI [5] reports that 56 out of 86 volunteers (i.e. 65%) were able to operate the appliance with a mean information transfer rate of 12.10±7.31 bit/min and accuracy of 89.16±9.29%. These results were obtained for a 5-way controller. In our case, all 8 responsive frequencies were needed to use the speller. Note, that in Fig. 5 the red boxplots, which outline the distributions of the AUC values for the 8 frequencies obtained for subjects not able to complete the tasks, span wide ranges. In such case, decreasing the number of frequencies needed to control the interface would allow to get rid of the least favourable frequencies, and hence most probably increase the fraction of population able to efficiently control the proposed system.

V. CONCLUSIONS

Novelty of the system proposed in this study relies on the direct use of phase-locking properties of the SSVEP responses in the formation of features, used for classification of

user decisions. The process of pattern formation can be understood in terms of comb-filtering of the input buffers, which are phase-synchronized to flickering stimuli. This type of filtering effectively attenuates all the activity which is not phase-locked to the stimulation. Moreover, it includes information from all the harmonics and their mutual phase relations. Improved efficiency of this scheme of SSVEP processing, as compared to detection based solely on the relative changes in spectral power, was hereby demonstrated on the same data. Overall, combination of hardware rendering and control of the stimuli parameters with novel approach to the parametrization of the SSVEP response seems to yield the fastest high-frequency SSVEP-BCI reported to date.

Communication via high-frequency SSVEP-based BCI was achieved only by 9 out of 15 (60%) participants of this study. While this ratio is in concordance with the previous reports on BCI literacy, in this case the difficulty was increased by requiring each user to produce reliable response in 8 frequencies from the 30–39 Hz range.

Information transfer rate was significantly higher in simpler task involving flat interface for direct choosing one of 8 available options (7-letter speller, with layout organized in the order of expected selection) compared to generic full-alphabet two-level interface. On the average, selection of each letter lasted 310 ms more in the generic interface. This suggests that efficiency of the BCI can be significantly improved by careful design of the interface layouts.

REFERENCES

[1] D. Regan, *Human Brain Electrophysiology: Evoked Potentials and Evoked Magnetic Fields*, 1989.

[2] F.-B. Vialatte, M. Maurice, J. Dauwels, and A. Cichocki, "Steady-state visually evoked potentials: Focus on essential paradigms and future perspectives," *Prog. Neurobiol.*, vol. 90, no. 4, pp. 418–438, Apr. 2010.

[3] R. Kuś *et al.*, "On the quantification of SSVEP frequency responses in human EEG in realistic BCI conditions," *PLoS ONE*, vol. 8, no. 10, p. e77536, 2013.

[4] C. S. Herrmann, "Human EEG responses to 1–100 Hz flicker: Resonance phenomena in visual cortex and their potential correlation to cognitive phenomena," *Exp. Brain Res.*, vol. 137, nos. 3–4, pp. 346–353, Apr. 2001.

[5] I. Volosyak, D. Valbuena, T. Lüth, T. Malechka, and A. Gräser, "BCI demographics II: How many (and what kinds of) people can use a high-frequency SSVEP BCI?" *IEEE Trans. Neural Syst. Rehabil. Eng.*, vol. 19, no. 3, pp. 232–239, Jun. 2011.

[6] C. Guger *et al.*, "How many people could use an SSVEP BCI?" *Frontiers Neurosci.*, vol. 6, p. 169, Nov. 2012.

[7] R. S. Fisher, G. Harding, G. Erba, G. L. Barkley, and A. Wilkins, "Photic- and pattern-induced seizures: A review for the Epilepsy Foundation of America Working Group," *Epilepsia*, vol. 46, no. 9, pp. 1426–1441, Sep. 2005.

[8] W. Yijun, W. Ruiping, G. Xiaorong, and G. Shangkai, "Brain-computer interface based on the high-frequency steady-state visual evoked potential," in *Proc. 1st Int. Conf. Neural Interface Control*, May 2005, pp. 37–39.

[9] P. J. Durka *et al.*, "User-centered design of brain-computer interfaces: OpenBCI.pl and BCI appliance," *Bull. Polish Acad. Sci.*, vol. 3, no. 3, pp. 427–433, 2012.

[10] I. Volosyak, D. Valbuena, T. Malechka, J. Peuscher, and A. Gräser, "Brain–computer interface using water-based electrodes," *J. Neural Eng.*, vol. 7, no. 6, p. 066007, Dec. 2010.

[11] Z. J. Koles, M. S. Lazar, and S. Z. Zhou, "Spatial patterns underlying population differences in the background EEG," *Brain Topogr.*, vol. 2, no. 4, pp. 275–284, 1990.

[12] J. O. Smith, III, "Physical audio signal processing: For virtual musical instruments and audio effects," in *Linear Predictive*. 2010.

[13] J. Fogarty, R. S. Baker, and S. E. Hudson, "Case studies in the use of ROC curve analysis for sensor-based estimates in human computer interaction," in *Proc. Graph. Interface*, 2005, pp. 129–136.

[14] H. Zhang, "The optimality of naive Bayes," *Proc. AA*, vol. 1, no. 2, p. 3, 2004.

[15] J. R. Wolpaw, H. Ramoser, D. J. McFarland, and G. Pfurtscheller, "EEG-based communication: Improved accuracy by response verification," *IEEE Trans. Rehabil. Eng.*, vol. 6, no. 3, pp. 326–333, Sep. 1998.

[16] Y. Wang, R. Wang, X. Gao, B. Hong, and S. Gao, "A practical VEP-based brain-computer interface," *IEEE Trans. Neural Syst. Rehabil. Eng.*, vol. 14, no. 2, pp. 234–239, Jun. 2006.

[17] Z. Lin, C. Zhang, W. Wu, and X. Gao, "Frequency recognition based on canonical correlation analysis for SSVEP-based BCIs," *IEEE Trans. Biomed. Eng.*, vol. 54, no. 6, pp. 1172–1176, Jun. 2007.

[18] P. F. Diez, V. A. Mut, E. M. A. Perona, and E. L. Leber, "Asynchronous BCI control using high-frequency SSVEP," *J. Neuroeng. Rehabil.*, vol. 8, p. 39, Jul. 2011.

[19] G. G. Molina and V. Mihajlovic, "Spatial filters to detect steady-state visual evoked potentials elicited by high frequency stimulation: BCI application," *Biomed. Techn.*, vol. 55, no. 3, pp. 173–182, Jun. 2010.

[20] G. G. Molina, D. Zhu, and S. Abtahi, "Phase detection in a visual-evoked-potential based brain computer interface," in *Proc. 18th Eur. Signal Process. Conf.*, 2010, pp. 949–953.

[21] P.-L. Lee *et al.*, "An SSVEP-actuated brain computer interface using phase-tagged flickering sequences: A cursor system," *Ann. Biomed. Eng.*, vol. 38, no. 7, pp. 2383–2397, Jul. 2010.

[22] D. Zhu, G. Garcia-Molina, V. Mihajlović, and R. M. Aarts, "Online BCI implementation of high-frequency phase modulated visual stimuli," in *Proc. Int. Conf. Universal Access Hum.-Comput. Interact.*, 2011, pp. 645–654.

[23] P. F. Diez *et al.*, "Commanding a robotic wheelchair with a high-frequency steady-state visual evoked potential based brain–computer interface," *Med. Eng. Phys.*, vol. 35, no. 8, pp. 1155–1164, Aug. 2013.

[24] J. Tong and D. Zhu, "Multi-phase cycle coding for SSVEP based brain-computer interfaces," *Biomed. Eng. Online*, vol. 14, no. 1, p. 5, 2015.